JACS
JOURNAL OF THE AMERICAN CHEMICAL SOCIETY

Article

pubs.acs.org/JACS

Formation of 3D Cholesterol Crystals from 2D Nucleation Sites in Lipid Bilayer Membranes: Implications for Atherosclerosis

Neta Varsano,[†] Iael Fargion,[†] Sharon G. Wolf,[‡] Leslie Leiserowitz,[§] and Lia Addadi*[,†]

[†]Department of Structural Biology, Weizmann Institute of Science, Rehovot 76100, Israel

[‡]Department of Chemical Research Support, Weizmann Institute of Science, Rehovot 76100, Israel

[§]Department of Materials and Interfaces, Weizmann Institute of Science, Rehovot 76100, Israel

Supporting Information

ABSTRACT: Atherosclerosis is the major precursor of cardiovascular disease. The formation of cholesterol crystals in atherosclerotic plaques is associated with the onset of acute pathology. The cholesterol crystals induce physical injury in the plaque core, promoting cell apoptosis and triggering an increased inflammatory response. Herein we address the question of how cholesterol crystal formation occurs in atherosclerosis. We demonstrate that three-dimensional (3D) cholesterol crystals can undergo directed nucleation from bilayer membranes containing two-dimensional (2D) cholesterol crystalline domains. We studied crystal formation on supported lipid bilayers loaded with exogenous cholesterol and labeled using a monoclonal antibody that specifically recognizes ordered cholesterol arrays. Our findings show that 3D crystals are formed exclusively on the bilayer regions where there are segregated 2D cholesterol crystalline domains and that they form on the domains. This study has potentially significant implications for our understanding of the crucial step in the mechanism by which atherosclerotic lesions form.

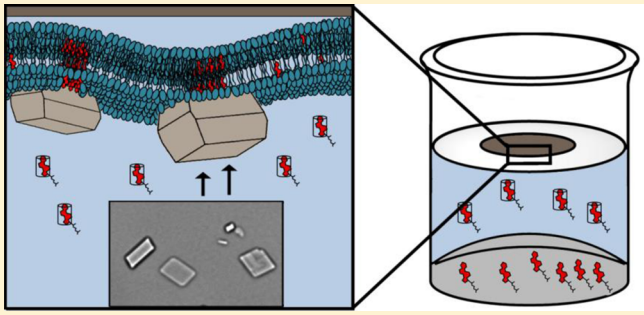

INTRODUCTION

The accumulation of lipids and cholesterol in plaques in the innermost layer of the artery wall is considered the hallmark of atherosclerosis.[1−4] Plaque rupture results in vascular occlusion, a precursor to cardiovascular diseases such as heart attack and stroke, the most common causes of death in Western societies.[5] The plaque is composed of macrophage cells and cell debris with underlying areas of cholesterol crystals.

Cholesterol is essential for animal cell life,[6] functioning in the maintenance of cell membrane structure and mechanical−dynamical properties.[7−9] The trafficking of cholesterol to peripheral tissues in the blood is carried out mainly by low density lipoprotein (LDL) particles; these consist of a triglyceride and esterified cholesterol core bound by a shell of phospholipids, cholesterol, and proteins.[10] In early stages of atherosclerosis, modified LDL particles trapped in the artery inner layer trigger an immune-system response. Macrophage cells recruited to the area accumulate cholesteryl ester and hydrolyze it to cholesterol, which is then delivered to the cell membrane. Subsequently, an imbalance between cholesterol uptake and cholesterol removal leads to high levels of cholesterol accumulation in so-called foam cells. This accumulation process eventually results in the formation of plaques[11] that are rich in cholesterol monohydrate crystals.[12]

Cholesterol crystal formation within the arterial wall is a practically nonreversible process. Even though in vitro studies have shown that cholesterol crystals can be in part eliminated by high density lipoprotein (HDL), this activity is limited in vivo.[13] Crystalline cholesterol thus accumulates, triggering increased inflammatory response, physical injury to cells, and acute progression of plaque disruption.[14−16]

Kruth et al.[17] showed that macrophages generate cholesterol crystalline domains in the cell membrane when an excess of cholesterol is induced by LDL particle fagocytosis. Ong et al.[18] subsequently discovered the presence of cholesterol particles in the vicinity of cell membranes in atherosclerotic plaques and in macrophage cell culture.

In parallel, Ziblat and co-workers[19−22] examined the conditions under which two-dimensional (2D) cholesterol crystalline domains are formed in supported lipid bilayers with different compositions of cholesterol (Chol) and sphingomyelin (SM), dipalmitoylphosphatidylcholine (DPPC), or ceramide (Cer), whose structures are shown in Figure 1B. A typical cholesterol concentration above which cholesterol segregates to form cholesterol 2D crystalline domains was determined for each mixture: SM/Chol at 38 ± 3 mol % cholesterol, DPPC/Chol at 54 ± 3 mol % cholesterol, and Cer/Chol at 45 ± 5 mol % cholesterol.[19−22] We note that SM and DPPC are known to form with cholesterol ordered nanodomains in cell membranes as well as in model lipid bilayers.[23−28]

Received: November 12, 2014
Published: January 13, 2015

DOI: 10.1021/ja511642t
J. Am. Chem. Soc. 2015, 137, 1601−1607

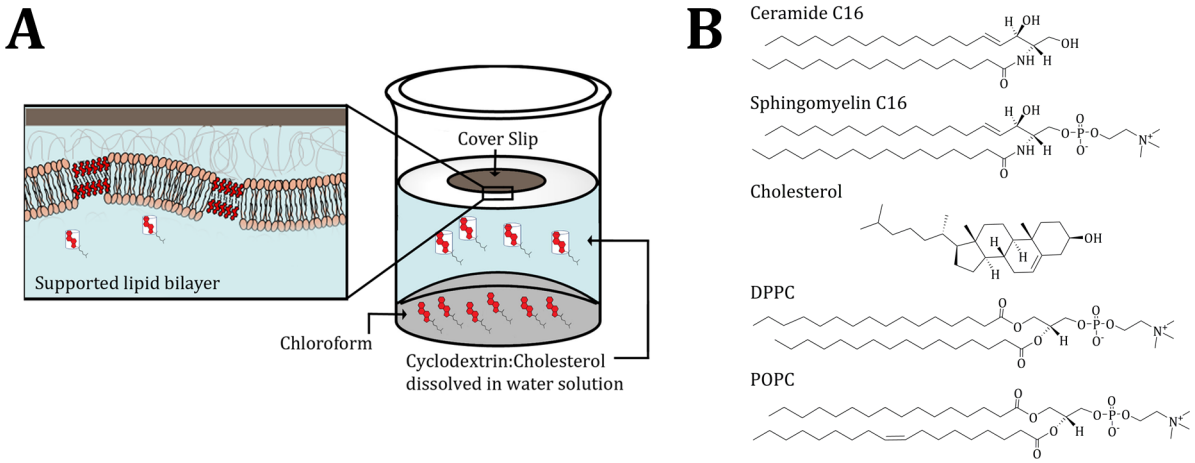

Figure 1. (A) Three-phase system for the delivery of exogenous cholesterol to the lipid bilayers. The supported lipid bilayer floats on an aqueous phase containing cholesterol complex. A saturated cholesterol solution in chloroform is placed below the water phase. (B) Chemical formulas of the lipids studied.

Cholesterol 2D crystalline domains pack in a rectangular crystal structure[29,30] different from that of the three-dimensional (3D) triclinic cholesterol monohydrate crystals found in atherosclerotic plaques.[12,31] Solomonov et al.[30] and Ziblat et al.[22] showed that the rectangular 2D phase of cholesterol can spontaneously transform into the triclinic 3D phase starting from lipid bilayers. These results, together with the data of Ong et al.,[18] led to the hypothesis that 2D crystalline domains of cholesterol in cell membranes may induce nucleation of the 3D crystals at early stages of atherosclerosis.

Here we check the viability of this hypothesis in vitro. Using a suitable external cholesterol delivery system, we show that different lipid bilayers can indeed nucleate 3D cholesterol crystals, but only when they contain 2D cholesterol crystalline domains.

RESULTS

The system for delivery of cholesterol to the lipid bilayers was constructed as a three-phase setup (Figure 1A). Supported lipid bilayers are deposited on coverslips by vesicle fusion.[22] The coverslips float on an aqueous phase containing a complex of cholesterol with the cholesterol carrier methyl-β-cyclodextrin (MβCD). A saturated cholesterol solution in chloroform is placed below the water phase. Cyclodextrin extracts cholesterol from the chloroform solution and delivers it to the bilayer.

Lipid bilayers composed of different lipid mixtures of cholesterol with the unsaturated glycerolipid palmitoyloleoylphosphatidylcholine (POPC), DPPC, and SM were studied (Table 1). POPC (40 mol %) was introduced into the DPPC and SM mixtures in order to stabilize the bilayers during the formation of curved vesicles and vesicle fusion (Table 1). Cholesterol has low solubility in POPC,[32−34] beyond which it segregates from POPC in distinct nanodomains. The lipid mixture POPC1 studied here, composed of 75% POPC and 25% cholesterol, is well beyond the segregation point, whereas POPC2 does not contain cholesterol domains at the beginning (Table 1). Analogously, two Chol/DPPC/POPC lipid bilayer mixtures and two Chol/SM/POPC mixtures were constructed such that DPPC1 and SM1 contained cholesterol crystalline domains from the beginning, whereas DPPC2 and SM2 did not[20,21] (Table 1).

Table 1. Lipid Bilayer Compositions Studied

	Chol (mol %)	DPPC (mol %)	SM (mol %)	POPC (mol %)
POPC1	25	0	0	75
POPC2	0	0	0	100
DPPC1	42	18	0	40
DPPC2	18	42	0	40
SM1	48	0	12	40
SM2	12	0	48	40

The supported bilayers POPC1, POPC2, DPPC1, and DPPC2 were incubated with a MβCD:cholesterol solution for 1.5, 2.5, or 3.5 h using the cholesterol delivery system described above. After incubation, the bilayers were labeled with the structural antibody 58B1, which specifically interacts with cholesterol 2D and 3D crystals but not with isolated cholesterol molecules.[35,36] Following incubation with secondary fluorescently labeled antibody, each set of supported bilayers was observed by epifluorescence microscopy. In order to avoid any influence of fluorescence decay on the results, all of the samples were imaged in parallel on the same day of the experiment and under the same conditions. The fluorescence images were analyzed for their average intensity.

The fluorescence signals, expressed as bright areas in the images, correspond to the presence of cholesterol 2D crystalline domains labeled by antibody 58B1. In Figure 2, the time course of cholesterol domain growth was followed for the four bilayers, with the starting fluorescence intensity arbitrarily defined as 1 and the subsequent values normalized to the initial ones. First and foremost, these results imply that the amounts of cholesterol 2D domains in the bilayers increased with time as a result of cholesterol delivery. The increase in cholesterol domains was clearly much steeper for DPPC1 and DPPC2 than for POPC1 and POPC2, apparently reflecting the greater affinity of cholesterol for DPPC relative to POPC. The fluorescence jumps observed after 3.5 h for DPPC2 and after 1.5 h for POPC2 reflect the sudden appearance of cholesterol domains, i.e., the beginning of cholesterol segregation. The fact that the time lapse for cholesterol domain segregation is much shorter for POPC2 relative to DPPC2 is due to the very low solubility of cholesterol in POPC. DPPC1 and POPC1, which had segregated cholesterol domains from the beginning (Figure 3A and Figure S1 in the Supporting Information) showed rather a progressive increase in the

DOI: 10.1021/ja511642t
J. Am. Chem. Soc. 2015, 137, 1601−1607

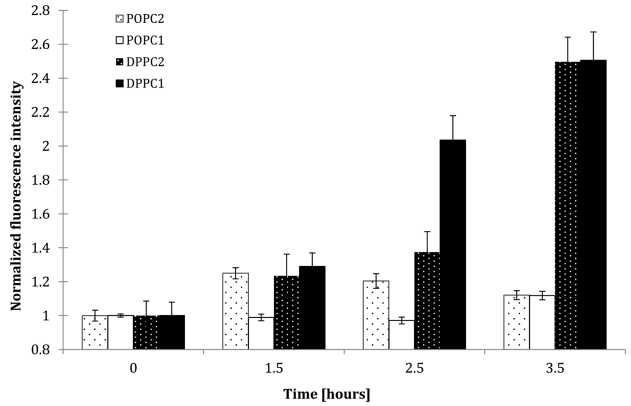

Figure 2. Time courses of segregated cholesterol domain appearance in the DPPC1, DPPC2, POPC1, and POPC2 bilayers. Data were analyzed using a computer algorithm that determines the average pixel intensity for each image. The starting point (t = 0) corresponds to bilayer membranes that were incubated with doubly distilled water. The fluorescence level at t = 0 for each bilayer was labeled as 1, and the subsequent measurements were normalized to this level. Data are shown as mean ± standard error.

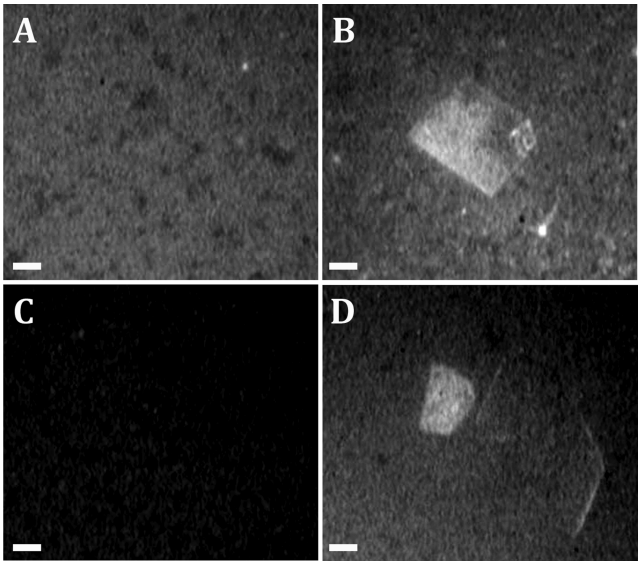

Figure 3. (A, C) Fluorescence micrographs of DPPC1 and DPPC2 bilayers, respectively, labeled with 58B1 antibody (1.5 μg/mL). (B, D) Fluorescence images of the bilayers in (A) and (C), respectively, after incubation with cholesterol for 5 h. Both the membranes and crystals were labeled. Scale bars in all images are 10 μm. The resolution of the fluorescence microscope (0.5 μm) is much lower than what would be needed to observe individual domains, which have diameters of a few tens of nanometers.

domain population. The increase was very slow for POPC1 and started to pick up only after 2.5 h. Interestingly, when the MβCD:cholesterol solution was put in touch with crystalline cholesterol deposited on the vial walls, the opposite cholesterol delivery profile was observed, i.e., MβCD extracted cholesterol from the lipid bilayers and delivered it to the crystals (Figure S2 in the Supporting Information). This implies that in contrast to cholesterol dissolved in chloroform, crystalline cholesterol is a preferred sink for cholesterol delivery from the cyclodextrin complex relative to the lipid bilayer mixtures.

Cholesterol delivery to the lipid bilayers was followed in time by cholesterol 3D crystal formation. Samples of DPPC1 and DPPC2 were labeled with the structural antibody 58B1 after 5 h of incubation with cholesterol (Figure 3B,D, respectively) and compared with samples labeled before incubation with cholesterol (Figure 3A,C, respectively). As expected, the samples before incubation with cholesterol showed antibody labeling of DPPC1 but not of DPPC2. After 5 h of incubation, large (~50 μm) crystals attached to bilayers of both DPPC1 and DPPC2 were detected. The crystals were associated with 2D cholesterol crystalline domains over their whole area (Figure 3B,D). In agreement with the results in Figure 2, loading bilayers with cholesterol for long time periods leads to segregation of cholesterol domains, and this subsequently leads to the formation of 3D crystals. Attempts to remove the 3D crystals from the bilayers by water immersion and sonication (for 1 h) failed, indicating that the first layers of the crystals strongly interact with the bilayers, possibly being embedded inside them.

When the same DPPC1 and DPPC2 bilayers were incubated with cholesterol for 3.5 h, small (~10 μm) cholesterol crystals were detected on DPPC1 (Figure 4E) but not on DPPC2 (Figure 4F). After 3.5 h of incubation, cholesterol crystalline domains were also more abundant in DPPC1 bilayers (Figure 4C) relative to DPPC2 bilayers (Figure 4D). No crystals were detected outside the bilayer-covered area or floating in solution or at the solution−air interface.

Similar results were obtained for the sets of lipid mixtures POPC1/POPC2 and SM1/SM2 (Figure 5 and Figure S1 in the Supporting Information). Bilayers of POPC1 and POPC2 were incubated with cholesterol in parallel for 3.5 h. Incubation of SM1 and SM2 bilayers with cholesterol was performed for 1.5 h. Crystals were detected only on the POPC1 and SM1 bilayers, which contained 2D crystalline domains in the initial compositions (Figure 5A,C). The crystal illumination in cross-polarized light was very weak in all of the samples, indicating that the crystals were extremely thin (Figure S3 in the Supporting Information).

The crystals grown on Chol/DPPC/POPC and Chol/SM/POPC bilayers adopted three different crystal morphologies. Most of the crystals had the classic parallelogram morphology with a dihedral angle of 100.8° (Figure 4E and Figure 5), characteristic of triclinic cholesterol monohydrate (001) crystal platelets (Figure 6B). Some crystals, however, had an elongated morphology, and some appeared as curved cylindrical particles (Figure S4 in the Supporting Information). These peculiar morphologies are reminiscent of the curved coiled ribbons observed during cholesterol crystallization from bile acids.[37] On DPPC1 bilayers, areas existed where the elongated morphology was dominant (Figure 7B). When the same samples were observed on the next day, however, the bilayer contained only the classic cholesterol crystal plates (Figure 7C).

To assign the crystal structures to the crystals formed, electron microscope grids upon which the lipid bilayers were deposited were incubated with cholesterol as described above. The grids were vitrified by plunging them into liquid ethane and observed by cryogenic transmission electron microscopy (cryo-TEM) in imaging and electron diffraction (ED) modes. The diffraction patterns obtained for most of the crystals (Figure 6C) are typical for triclinic cholesterol monohydrate crystals on the [001] zone axis.[37] However, we identified another type of crystal diffraction that corresponds to a monoclinic structure with the reflections of d_{202} = 5 Å and d_{111} = 5.9 Å (Figure 7E). The appearance of the (111) and (202) diffractions in the [001] zone axis further confirmed the

DOI: 10.1021/ja511642t
J. Am. Chem. Soc. 2015, 137, 1601−1607

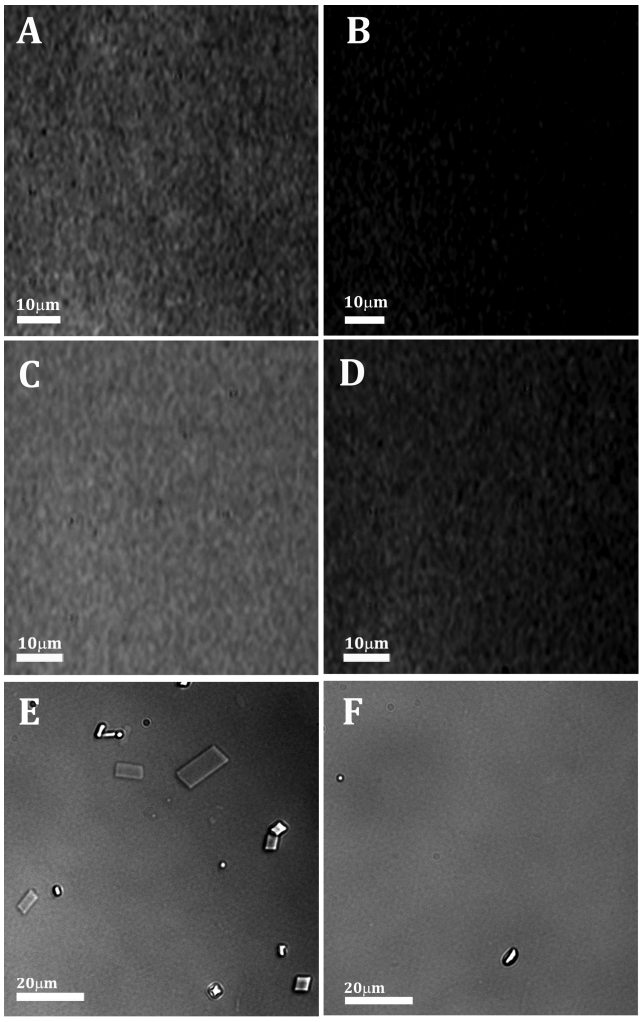

Figure 4. (A, B) Fluorescence images of DPPC1 and DPPC2 bilayers, respectively, labeled with 58B1 antibody (1.5 μg/mL). (C, D) Fluorescence images of the bilayers in (A) and (B), respectively, after incubation with cholesterol for 3.5 h. (E, F) White-light images of the bilayers in (C) and (E), respectively. Only the DPPC1 bilayer (E) showed the development of crystals. The speckle in (F) was not a crystal; it was kept to prove that the image was in focus.

extreme thinness of the crystals (Figure 7). Such electron diffraction from 3D crystals of the monoclinic form was previously observed once, in the 3D monoclinic crystals formed from mixtures of cholesterol with biliary acids.[37]

DISCUSSION

We have demonstrated here that bilayers containing cholesterol 2D crystalline domains can nucleate cholesterol 3D crystals from mixtures composed of Chol/POPC, Chol/SM/POPC, and Chol/DPPC/POPC. We have observed that the cholesterol content in DPPC and POPC bilayers increases with the delivery of exogenous cholesterol by cyclodextrin (Figure 2). DPPC1 bilayers, which contained segregated cholesterol domains from the start, promoted cholesterol 3D crystal formation after 3.5 h (Figure 4). In contrast, DPPC2 bilayers, which started to develop segregated cholesterol domains after 3.5 h, promoted cholesterol 3D crystal formation only after 5 h (Figures 3 and 4). This indicates that when cholesterol forms a homogeneous solution with other lipids, crystal nucleation does not occur. Cholesterol 3D crystals were

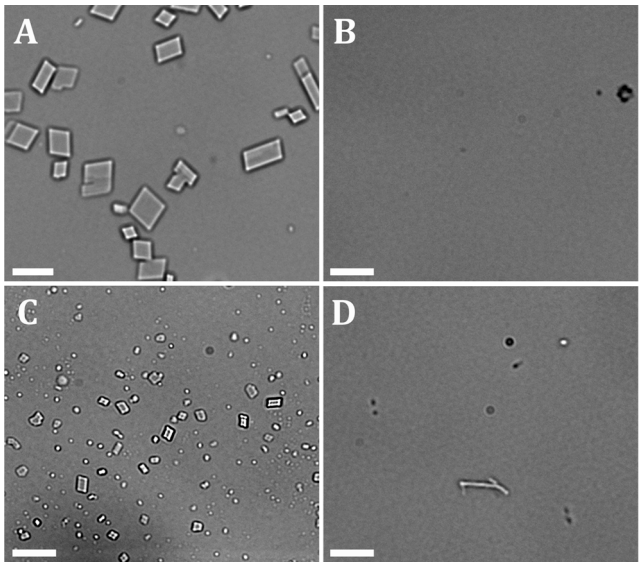

Figure 5. (A, B) Light microscope images of POPC1 and POPC2 bilayers, respectively, after incubation with cholesterol for 3.5 h. (C, D) Light images of SM1 and SM2 bilayers, respectively, after incubation with cholesterol for 1.5 h. Scale bars in all images are 10 μm.

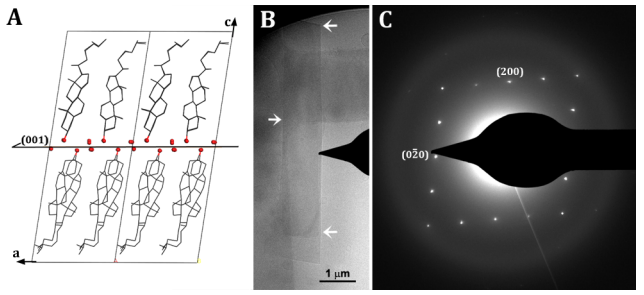

Figure 6. (A) Schematic showing two unit cells of a triclinic cholesterol monohydrate crystal viewed along the *b* axis. The H atomic positions are not marked. Gray, carbon; red, oxygen. The structure parameters were taken from ref 31. (B) Cryo-TEM image of a cholesterol monohydrate crystal. The arrows mark the edges of the crystal. (C) Cryo-ED pattern of the crystal presented in (B), demonstrating the classic triclinic cholesterol monohydrate diffraction pattern on the [001] zone axis. The crystals were grown with association to DPPC1 bilayers after 3.5 h of incubation with cholesterol.

not formed on POPC2 bilayers after 3.5 h, although cholesterol domains segregated after 1.5 h. However, the delivery of exogenous cholesterol to POPC is extremely slow relative to DPPC and was evidently not sufficient to produce 3D crystals (Figures 2 and Figure 5B). The intrinsically low affinity of cholesterol for incorporation into POPC bilayers, relative to the higher affinity for incorporation into DPPC bilayers, reflects the known tendency of DPPC to form mixed phases with cholesterol.[20,23,24,38,39] The affinity of cholesterol for incorporation into SM bilayers should be even higher because of the known tendency of cholesterol to function as a spacer between the SM backbone chains with bulky headgroups (the so-called "umbrella effect").[19,40−43] This might explain why the time scale for cholesterol crystal formation was much shorter for cholesterol/SM mixtures than for mixtures with POPC or DPPC (1.5 h relative to 3.5 h).

A decrease in crystalline domain population was observed when the lipid bilayer mixtures were incubated with cyclo-

DOI: 10.1021/ja511642t
J. Am. Chem. Soc. 2015, 137, 1601−1607

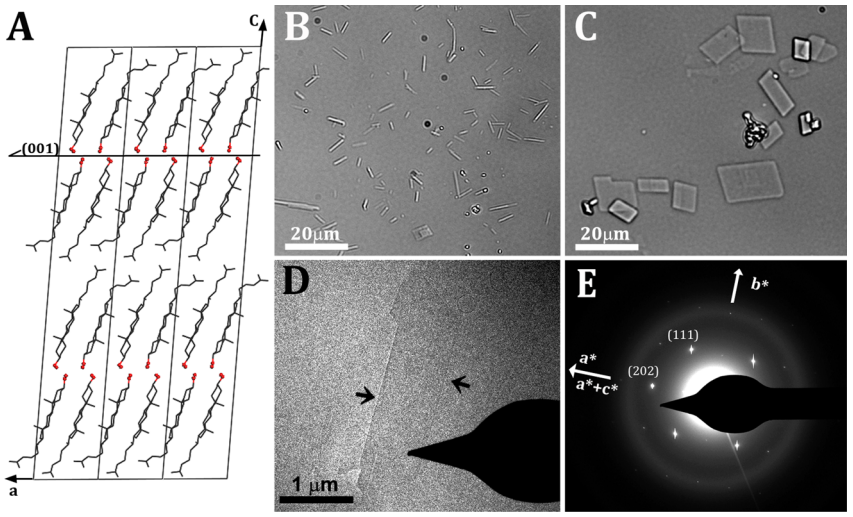

Figure 7. (A) Structure of three unit cells of a monoclinic cholesterol monohydrate crystal viewed along the *b* axis. The H atomic positions are not marked. Gray, carbon; red, oxygen. The structure parameters were taken from ref 30. (B, C) DPPC1 bilayers after incubation with cholesterol for 3.5 h. Images of the samples were taken the same day of the incubation (B) and on the next day (C). Long, narrow structures were the dominant feature in the first few hours post incubation. The parallelogram-shaped plate crystals were the dominant structure the next day. (D) Cryo-TEM image of a cholesterol crystal grown in association with DPPC1 bilayers after 3.5 h of incubation with cholesterol. (E) Cryo-ED pattern of the crystal in (D). The (202) and (111) reflections with d_{202} = 5 Å and d_{111} = 5.9 Å were indexed according to refs 30 and 37. These reflections, which do not belong to the [001] zone axis, became visible because of the extreme thinness of the crystal and the low angle between a^* and (a^* + c^*) (4.2°).

dextrin:cholesterol complex in competition with cholesterol crystals. This behavior stresses the tendency of cholesterol to grow by secondary nucleation on its own crystal template rather than being incorporated into the lipid bilayer.

The formation of 3D monoclinic crystals is a clear indication of nucleation from the rectangular 2D crystalline domains in the bilayer. Solomonov et al.[30] showed that even though the cholesterol rectangular motif is preferred in a bilayer, it is unfavorable in multilayers, where the triclinic structure is stabilized by the favorable hydrogen-bonding arrangement. A model for the single-crystal-to-single-crystal transition from the bilayer monoclinic phase to the stable triclinic 3D crystal was then suggested.[30] Similar spontaneous transformations between the two crystal phases were observed in two independent studies that were performed in supported lipid bilayers[22] and human bile vesicles.[37] The main difference between the experiments of Solomonov et al. and those reported here is that in the former cholesterol was endogenous to the bilayer, whereas in the latter it was exogenous. This raises the possibility, especially relevant in relation to the pathological scenario, that exogenous cholesterol aggregates may nucleate on the bilayer 2D cholesterol domains. A good lattice match exists over a limited region in the water molecule positions between the monoclinic and the triclinic phases on the (001) plane. This may favor templated nucleation of the triclinic phase on the 2D rectangular domains corresponding to the 3D monoclinic phase. At the present stage, we can conclude that both templated nucleation and phase transformation are possible scenarios. In any case, the two scenarios have the same outcome, i.e., formation of cholesterol crystals from cholesterol 2D domains in the membrane.

It appears that in the mixed systems where DPPC or SM was present together with 40% POPC, the major sites for cholesterol accumulation, segregation, and 3D crystal nucleation were in the cholesterol/DPPC or cholesterol/SM domains. This was also supported by the transient formation of curved particles similar to those formed by cholesterol with bile acids,[37] which was observed here in the presence of DPPC or SM but not with POPC alone. However, we cannot exclude the possibility that POPC may be actively involved in areas at the boundaries of ordered domains of cholesterol/DPPC/SM, participating in structures that do not exist in the absence of the saturated lipids.

The model system studied here, although drastically simplified, may have direct biological relevance. The formation of ordered domains of cholesterol with sphingolipids (represented here by SM) and saturated glycerolipids (represented by DPPC) is well-established in cell membranes.[24,27,28,44] Elevation of SM in aortic tissue has been directly related to the severity of atherosclerosis, and SM was found to be present in liposomes with high levels of cholesterol isolated from atherosclerotic plaques.[45,46] This process is thought to reflect not only the high affinity between cholesterol and SM but also an activated mechanism designed to stabilize cholesterol.[46] We suggest that stabilization may occur by formation of mixed domains, thus preventing cholesterol segregation.

In conclusion, the results reported here strengthen the hypothesis that cholesterol 2D crystalline domains segregated inside cell membranes may be associated with cholesterol crystal nucleation in the early stages of atherosclerosis, analogous to the process of cholesterol 3D crystal formation observed in model lipid bilayers and model bile solutions.[47] This hypothesis can further our understanding of the initiation of atherosclerotic lesions. By clarifying the critical pathological step of cholesterol nucleation, we can open the way for investigations of how to inhibit atherosclerosis at early stages.

EXPERIMENTAL SECTION

Materials. Cholesterol monohydrate (Avanti Polar Lipids, Birmingham, AL; cat. no. 700000P) was recrystallized before use for each experiment. The recrystallization procedure was developed in our lab and is described elsewhere.[35] Briefly, cholesterol (0.3 g) was added to 80 mL of boiling acetone. Doubly distilled water (DDW) (20 mL) was added to the solution, which was then boiled for another 30 s and

DOI: 10.1021/ja511642t
J. Am. Chem. Soc. 2015, 137, 1601−1607

cooled to room temperature. After a few hours, a white cloudy suspension formed; the solution was shaken vigorously and left overnight at room temperature. The solution was filtered, and the filtrate was left at 4 °C for 3 days. The pure crystals were filtered and kept at −20 °C under a nitrogen atmosphere.

Rhodamine TRITC-AffiniPure donkey anti-mouse IgM, μ-chain specific, was obtained from Jackson ImmunoResearch Laboratories (cat. no. 115-025-020). Lipids were obtained from Avanti Polar Lipids: DPPC (cat. no. 850355P), SM (cat. no. 860062C), and POPC (cat. no. 850457C). All of the lipids were used without further purification, and 10^{-3} M stock solutions of lipids in chloroform were stored at −20 °C until use. MβCD was obtained from Sigma (cat. no. C-4555) and kept sealed at room temperature until use.

Vesicle Formation. Vesicles with the desired lipid molar ratios (42:18:40 and 18:42:40 Chol/DPPC/POPC, 48:12:40 and 12:48:40 Chol/SM/POPC, 25:75 Chol/POPC, and 100% POPC) were prepared following a procedure described elsewhere.[22] Briefly, 0.14 mg of the desired lipid mixture was prepared by mixing the appropriate amounts of lipid dissolved in chloroform. The mixture was added into an Eppendorf tube (2 mL) and dried by nitrogen flux to obtain a lipid film on the walls of the Eppendorf tube. The film was kept under vacuum for at least 15 min and then hydrated with 1 mL of Milli-Q-grade water. The suspension was then heated above the lipid transition temperature and mixed by vortex in three cycles (3 min each). Five additional cycles were performed in which each step involved freezing the suspension in liquid nitrogen and heating it above the lipid transition temperature (5 min each). In order to get unilamellar vesicles, the suspension was then extruded nine times through a polycarbonate membrane with a pore diameter of 0.1 μm (Avanti Polar Lipids) at a temperature higher than the lipid transition temperature.

Preparation of Supported Lipid Bilayers. Glass slides (Thermo Scientific Menzel-Gläser, 13 mm diameter and 0.13−0.16 mm thick) were cleaned extensively by boiling in *n*-hexane, acetone, and ethanol, with each immersion lasting 5 min. The glasses were immersed in piranha solution for 20 min, followed by three washes with DDW. In order to achieve an hydrophilic "cushion" surface, the glasses were immersed in 1000 ppm polyethyleneimine (PEI) (Polysciences, Warrington, PA) solution overnight.[48] Vesicle suspensions were spread on the hydrophilic glasses such that the final lipid concentration was 0.14 mg/mL in DDW. The sample was heated above the lipid transition temperature for 15−20 min to allow the spontaneous process of vesicle adhesion, fusion, and rupture to take place on the surface. The samples were washed three times with DDW to remove unruptured vesicles. For TEM experiments, the same procedure was performed on Quantifoil S 7/2 200 mesh nickel TEM grids (see the cryo-TEM procedure below).

Antibody Purification. The monoclonal 58B1 antibodies were purified from the supernatant hybridoma fluid by affinity chromatography using an ImmunoPure IgM purification kit according to the manufacturer's instructions. The purified fractions were checked by UV absorbance at 280 nm, and those with optical density higher than 0.2 were collected and dialyzed (Spectra/Por membrane with cutoff 12000−14000 Da) in 2 L of phosphate-buffered saline (PBS) at 4 °C (the PBS solution was changed three times every 4 h). The antibodies were used for a maximum of 5 days after purification. The antibody concentration was checked by UV absorbance at 280 nm each day before use.

Immunofluorescence. Lipid bilayers were deposited on glass coverslips and incubated with the antibodies at a concentration of 1.5 μg in 1 mL of DDW for 20 min. The samples were then washed three times and incubated with fluorescent secondary antibody (see Materials) at a concentration of 12 μg in 1 mL of DDW for 20 min. After another three washes, the samples were observed under a Zeiss epifluorescence microscope with a rhodamine filter (575 nm). The microscope was equipped with a video camera attached to a LIS-700 integration amplifier (Applitec, Holon, Israel).

All of the samples in each experimental set were prepared and examined in parallel under the same conditions while keeping the imaging parameters (exposure and signal gain) constant. Each bilayer system was tested at least three times with reproducible results. For each sample, five to seven images were recorded in different areas of the glass, of which average representative images are presented. The fluorescence intensity was evaluated using ImageJ software.

Cyclodextrin:Cholesterol Complex. Cyclodextrin:cholesterol complex was prepared as described previously.[49] Briefly, a thin layer of cholesterol was deposited on the walls of a round flask by drying under a nitrogen flux a solution of 0.8 mg cholesterol dissolved in chloroform/methanol 1:1 (v/v). A solution of 33.45 mg of MβCD dissolved in 10 mL of water was added to the dried layer, and the mixture was vortexed for 1 min. The flask was then placed in a water bath sonicator until a clear solution was achieved. The saturated MβCD:cholesterol solution was placed in a rotating incubator at 37 °C overnight to yield a final 2.5 mM MβCD:cholesterol solution. Immediately before use, the solution was filtered through a 0.45 μM syringe filter (Millipore, Bedford, MA).

Lipid Bilayer Incubation with Cyclodextrin:Cholesterol Complex. A saturated solution of cholesterol in chloroform (100 μL) was injected into 6 mL of MβCD:cholesterol solution, resulting in a two-phase system. The coverslip with the deposited lipid bilayer was placed floating on the aqueous solution with the bilayer facing down into the solution. In order to ensure that the coverslip would float through the entire incubation time, a supported Teflon sheet was used (Figure 1). After incubation with such a cholesterol-rich environment, the coverslip was immersed in water and washed three times.The samples were observed by light microscopy (Nikon ECLIPSE E600 POL) or fluorescence microscopy as needed.

Cryo-TEM. Quantifoil S 7/2 200 mesh nickel TEM grids (Quantifoil Micro Tools, Jena, Germany) were glow-discharged for 60 s (EMS glow-discharge apparatus) and then immediately immersed in solutions of 1000 ppm PEI for 20 min. Vesicle suspensions were spread on the hydrophilic grid surface to form supported lipid bilayers following the vesicle fusion procedure described above. The grids were then incubated with the cholesterol delivery system. At the end of the incubation, the grids were washed with DDW, blotted, and immediately plunged into liquid ethane (Leica EM-GP plunger, Leica Microsystems).

Frozen samples were transferred to a Gatan 626 cryoholder, maintaining the sample temperature below −176 °C inside the microscope. Samples were observed with an FEI Tecnai F-20 transmission electron microscope (FEI Corporation, Hillsboro, OR) operating at 200 kV. Images and diffraction patterns were recorded on a Gatan US4000 CCD camera (Gatan Inc., Pleasanton, CA) using low-dose conditions.

■ ASSOCIATED CONTENT

Ⓢ Supporting Information

Cholesterol domain growth over time in Chol/POPC and POPC bilayers (Figure S1); graph of cholesterol domain growth with time using different cholesterol delivery systems (Figure S2); different cholesterol crystal morphologies grown on Chol/DPPC/POPC bilayers (Figure S3); and cholesterol crystals under crossed polarizers (Figure S4). This material is available free of charge via the Internet at http://pubs.acs.org.

■ AUTHOR INFORMATION

Corresponding Author

*lia.addadi@weizmann.ac.il

Notes

The authors declare no competing financial interest.

■ ACKNOWLEDGMENTS

This research was supported by the Binational Science Foundation (Grant 2013045). All of the EM studies were conducted at the Irving and Cherna Moskowitz Center for Nano and Bio-Nano Imaging at the Weizmann Institute of

DOI: 10.1021/ja511642t
J. Am. Chem. Soc. 2015, 137, 1601−1607

Science. L.A. is the incumbent of the Dorothy and Patrick Gorman Professorial Chair of Biological Ultrastructure.

REFERENCES

(1) Insull, W., Jr.; Bartsch, G. *J. Clin. Invest.* **1966**, *45*, 513.
(2) Kruth, H. S. *Am. J. Pathol.* **1984**, *114*, 201.
(3) Kruth, H. S. *Curr. Mol. Med.* **2001**, *1*, 633.
(4) Katz, S.; Shipley, G. G.; Small, D. *J. Clin. Invest.* **1976**, *58*, 200.
(5) Go, A. S.; Mozaffarian, D.; Roger, V. L.; Benjamin, E. J.; Berry, J. D.; Blaha, M. J.; Dai, S.; Ford, E. S.; Fox, C. S.; Franco, S. *Circulation* **2014**, *129*, e28.
(6) Alberts, B.; Johnson, A.; Lewis, J.; Raff, M.; Roberts, K.; Walter, P. *Molecular Biology of the Cell*, 4th ed.; Garland Science: New York, 2002.
(7) Simons, K.; van Meer, G. *Biochemistry* **1988**, *27*, 6197.
(8) McMullen, T. P.; Lewis, R. N.; McElhaney, R. N. *Curr. Opin. Colloid Interface Sci.* **2004**, *8*, 459.
(9) van Meer, G.; Voelker, D. R.; Feigenson, G. W. *Nat. Rev. Mol. Cell Biol.* **2008**, *9*, 112.
(10) Crook, M. *Clinical Chemistry and Metabolic Medicine*, 7th ed.; Hodder Arnold: London, 2006.
(11) Kruth, H. S. *Front. Biosci.* **2001**, *6*, D429.
(12) Small, D. M.; Bond, M. G.; Waugh, D.; Prack, M.; Sawyer, J. *J. Clin. Invest.* **1984**, *73*, 1590.
(13) Adams, C.; Abdulla, Y. *Atherosclerosis* **1978**, *31*, 465.
(14) Small, D. *Arterioscler., Thromb., Vasc. Biol.* **1988**, *8*, 103.
(15) Rajamäki, K.; Lappalainen, J.; Öörni, K.; Välimäki, E.; Matikainen, S.; Kovanen, P. T.; Eklund, K. K. *PloS One* **2010**, *5*, No. e11765.
(16) Shah, P. K.; Falk, E.; Badimon, J. J.; Fernandez-Ortiz, A.; Mailhac, A.; Villareal-Levy, G.; Fallon, J. T.; Regnstrom, J.; Fuster, V. *Circulation* **1995**, *92*, 1565.
(17) Kruth, H. S.; Ifrim, I.; Chang, J.; Addadi, L.; Perl-Treves, D.; Zhang, W.-Y. *J. Lipid Res.* **2001**, *42*, 1492.
(18) Ong, D. S.; Anzinger, J. J.; Leyva, F. J.; Rubin, N.; Addadi, L.; Kruth, H. S. *J. Lipid Res.* **2010**, *51*, 2303.
(19) Ziblat, R.; Kjaer, K.; Leiserowitz, L.; Addadi, L. *Angew. Chem., Int. Ed.* **2009**, *48*, 8958.
(20) Ziblat, R.; Leiserowitz, L.; Addadi, L. *J. Am. Chem. Soc.* **2010**, *132*, 9920.
(21) Ziblat, R.; Leiserowitz, L.; Addadi, L. *Angew. Chem., Int. Ed.* **2011**, *50*, 3620.
(22) Ziblat, R.; Fargion, I.; Leiserowitz, L.; Addadi, L. *Biophys. J.* **2012**, *103*, 255.
(23) Stottrup, B. L.; Keller, S. L. *Biophys. J.* **2006**, *90*, 3176.
(24) Hancock, J. F. *Nat. Rev. Mol. Cell Biol.* **2006**, *7*, 456.
(25) Estep, T.; Mountcastle, D.; Barenholz, Y.; Biltonen, R.; Thompson, T. *Biochemistry* **1979**, *18*, 2112.
(26) Bach, D.; Wachtel, E. *Biochim. Biophys. Acta* **2003**, *1610*, 187.
(27) Hanzal-Bayer, M. F.; Hancock, J. F. *FEBS Lett.* **2007**, *581*, 2098.
(28) Marsh, D. *Biochim. Biophys. Acta* **2009**, *1788*, 2114.
(29) Rapaport, H.; Kuzmenko, I.; Lafont, S.; Kjaer, K.; Howes, P. B.; Als-Nielsen, J.; Lahav, M.; Leiserowitz, L. *Biophys. J.* **2001**, *81*, 2729.
(30) Solomonov, I.; Weygand, M. J.; Kjaer, K.; Rapaport, H.; Leiserowitz, L. *Biophys. J.* **2005**, *88*, 1809.
(31) Craven, B. M. *Nature* **1976**, *260*, 727.
(32) Reyes Mateo, C.; Ulises Acuna, A.; Brochon, J.-C. *Biophys. J.* **1995**, *68*, 978.
(33) de Almeida, R. F.; Fedorov, A.; Prieto, M. *Biophys. J.* **2003**, *85*, 2406.
(34) Halling, K. K.; Ramstedt, B.; Nyström, J. H.; Slotte, J. P.; Nyholm, T. K. *Biophys. J.* **2008**, *95*, 3861.
(35) Perl-Treves, D.; Kessler, N.; Izhaky, D.; Addadi, L. *Chem. Biol.* **1996**, *3*, 567.
(36) Izhaky, D.; Addadi, L. *Adv. Mater.* **1998**, *10*, 1009.
(37) Weihs, D.; Schmidt, J.; Goldiner, I.; Danino, D.; Rubin, M.; Talmon, Y.; Konikoff, F. M. *J. Lipid Res.* **2005**, *46*, 942.
(38) Ege, C.; Ratajczak, M. K.; Majewski, J.; Kjaer, K.; Lee, K. Y. C. *Biophys. J.* **2006**, *91*, L01.
(39) Lange, Y.; Tabei, S. A.; Ye, J.; Steck, T. L. *Biochemistry* **2013**, *52*, 6950.
(40) Veatch, S. L.; Keller, S. L. *Phys. Rev. Lett.* **2005**, *94*, No. 148101.
(41) Slotte, J. P. *Chem. Phys. Lipids* **1999**, *102*, 13.
(42) Sankaram, M. B.; Thompson, T. E. *Biochemistry* **1990**, *29*, 10670.
(43) Collado, M. I.; Goñi, F. M.; Alonso, A.; Marsh, D. *Biochemistry* **2005**, *44*, 4911.
(44) Brown, D. A.; London, E. *Biochem. Biophys. Res. Commun.* **1997**, *240*, 1.
(45) Böttcher, C.; Van Gent, C. *J. Atheroscler. Res.* **1961**, *1*, 36.
(46) Chao, F.-F.; Blanchette-Mackie, E. J.; Dickens, B.; Gamble, W.; Kruth, H. S. *J. Lipid Res.* **1994**, *35*, 71.
(47) Frincu, M. C.; Fleming, S. D.; Rohl, A. L.; Swift, J. A. *J. Am. Chem. Soc.* **2004**, *126*, 7915.
(48) Wong, J. Y.; Majewski, J.; Seitz, M.; Park, C. K.; Israelachvili, J. N.; Smith, G. S. *Biophys. J.* **1999**, *77*, 1445.
(49) Christian, A.; Haynes, M.; Phillips, M.; Rothblat, G. *J. Lipid Res.* **1997**, *38*, 2264.

DOI: 10.1021/ja511642t
J. Am. Chem. Soc. 2015, 137, 1601−1607